

# We are IntechOpen, the world's leading publisher of Open Access books Built by scientists, for scientists

6,900

Open access books available

186,000

International authors and editors

200M

Downloads

Our authors are among the

154

Countries delivered to

TOP 1%

most cited scientists

12.2%

Contributors from top 500 universities



WEB OF SCIENCE™

Selection of our books indexed in the Book Citation Index  
in Web of Science™ Core Collection (BKCI)

Interested in publishing with us?  
Contact [book.department@intechopen.com](mailto:book.department@intechopen.com)

Numbers displayed above are based on latest data collected.  
For more information visit [www.intechopen.com](http://www.intechopen.com)



---

## Morphing Technologies: Adaptive Ailerons

---

Ignazio Dimino, Gianluca Amendola,  
Francesco Amoroso, Rosario Pecora and  
Antonio Concilio

Additional information is available at the end of the chapter

<http://dx.doi.org/10.5772/63645>

---

### Abstract

European Union is involving increasing amount of resources on research projects that will dramatically change the costs of building and operating aircraft in the near future. Morphing structures are a key to turn current airplanes to more efficient and versatile means of transport, operating into a wider range of flight conditions.

The concept of morphing may aim at a large number of targets, and its assessment strongly depends on the final objectives and the components where it has to be deployed. Maneuver, takeoff, landing, cruise conditions, just to cite few and very general examples, have all their own peculiarities that drive the specifications the wing shape change has to suit on.

In general, an adaptive structure ensures a controlled and fully reversible transition from a baseline shape to a set of different configurations, each capable of withstanding the relative external loads. The level of complexity of morphing structures naturally increases as a consequence of the augmented functionality of the reference system. Actuation mechanisms constitute a very crucial aspect for adaptive structures design because has to comply variable wing shapes with associated loads and ensure the prescribed geometrical envelope.

This chapter provides a presentation of the state of the art, technical requirements, and future perspectives of morphing ailerons. It addresses morphing aircraft component architecture and design with a specific focus on the structural actuator system integration. The approach, including underlying concepts and analytical formulations, combines methodologies and tools required to develop innovative air vehicles. Aileron is a very delicate region, where aeroelastic phenomena may be very important because of the very reduced local stiffness and the complex aerodynamics, typical of the wingtip zone. On the other side, this wing segment showed to be the one where higher cruise benefits could be achieved by local camber variations. This target was achieved while keeping the typical maneuver functions.

**Keywords:** morphing, actuation systems, distributed actuation, wind tunnel tests, aileron, lift control

---

## 1. Introduction

Men desired to flight since very ancient times being inspired by bird's capability to dominate sky. Nature offers a rich seam of inspiration for a new generation of morphing wing design across a wide range of scales of interest to engineers going from the biggest birds to the smallest insect. For example, birds achieve their wing morphing capability using flexible lifting surfaces, stiffened by hollow bones attached to strong muscle. All the flying creatures of the world show an inherent capacity to adapt, in a fraction of a second, their wing shape as the flight condition changes. A very interesting example may be represented by the perching sequence of an eagle. As reported in [1], birds accomplish changes in wingspan and area by firstly flexing their wings, and then adopting a characteristic M-shape planform with the inner wing section sweeps forward, and the outer section sweeps backwards.

It is noteworthy that "inspiration from nature" is the keywords that lie behind any morphing idea. Many researchers and engineers around the world have been inspired by the multitasking flight capabilities of birds, which tend to cover a broad range of mission phases ranging from slow, near-hover flight to aggressive dives, in order to develop innovative methodologies involved to resolve many technological problems. Just only observing birds and other flying creature wings, it is possible to appreciate the complexity of such systems showing intrinsic capacities to adapt instinctively and immediately to the environment. In particular, birds are able to articulate their wings in a craning motion to vary the dihedral or sweep angles [1], wing area, wing planform, wingspan, and other parameters. These changes allow the bird to quickly adapt between soaring, cruising, and descending flight [1].

The morphing idea was well known by the engineering since the beginning of aviation such as the Wright brothers who built the "first heavier than air aircraft with engine" with twisted wing for roll control. Despite the past century of innovation in aircraft technology, the versatility of modern aircraft remains far worse than airborne biological counterparts. The shape modification accomplished by birds stands as one of the few examples of true morphing. As such, the aircraft engineers worldwide are devoting extensive effort to integrate these concepts in advanced mechanical systems in order to bring morphing technology to the readiness level of a flight vehicle. The key purpose is to realize an innovative device capable to adapt itself to the external environment conditions, by exhibiting an intrinsic multidisciplinary attitude involving structures, actuation, sensing, and control. In recent years, European community funded many research program involved to improve the morphing structures technology readiness level. SARISTU [2] (acronym of Smart Intelligent Aircraft Structures) was probably the most advanced large-scale integrating project on morphing structures, coordinated by Airbus, aiming at achieving reductions in aircraft weight and operational costs, as well as an improvement in the flight profile specifically related to aerodynamic performance. Ended in 2015, the project consisted of a joint integration of different conformal morphing concepts in a laminar wing with the aim to improve aircraft performance through a 6% drag reduction inside the lift coefficient range usually devoted to cruise, with a positive effect on fuel consumption. The final product of the project was the first full-scale completely morphing wing tip prototype, ever assembled in Europe, at Finmeccanica Headquarters (Pomigliano,

Italy), **Figure 1**. The innovative seamless morphing wing incorporates a gapless morphing leading edge, a morphing trailing edge, and an adaptive winglet.



**Figure 1.** Assembly of the SARISTU morphing wing consisting of different morphing devices [2].

Morphing technology is now approaching the high maturity practices for the integration on real aircraft. *How to adapt* is a problem regarding sensing, actuation, and control laws, which are very critical. Hence, although an animal's wings may be able to change shape in a complex manner, the total number of independently controlled degrees of freedom may not be high. This indicates that a smart structure is built upon relatively simple principles. It will be actuated in one point and, by means of movable structural elements with limited DOF; the movement is transmitted to the whole structure so that the wing will be built to adapt at loading rather than to resist it.

### 1.1. Actuation systems for morphing applications

The state of the art of high-lift actuation systems of aircraft control surfaces predominantly consists of mechanical transmission shafts moved by rotary or linear hydraulic actuators with common control valves. These architectures assure a synchronous, safe, and reliable deployment of all HLD (High Lift Device) but with limited flexibility [3]. The main functionality of the high-lift devices is to provide lift increment at low-speed condition (take/off and landing) so that the clean wing is optimized for the cruise speed regime. There are a lot of HLD on wing aircraft such as plain flaps to fowler flaps with single, double, and even the most complex triple slots (Boeing 747). The design and optimization of high-lift systems are one of the most complex tasks in aircraft design. It involves a close coupling of aerodynamics, structures, and kinematics. The evolutionary trend of the HLD has been strongly driven by the dramatic improvement in aerodynamic tools optimization and in computational systems for complex structure simulations (multi-body kinematics). At the early stage, the research of aerodynamics high-

lift performance ( $C_{Lmax}$ ) was achieved by means of multi-slotted experimentally validated two-dimensional flap design. These systems allowed to achieve satisfactory performance with penalties in structural complexity and weight and, therefore, in costs that were not sustainable in the current applications. Later on, the improvement in computation fluid dynamics has permitted to carefully optimize flap systems in two-dimensional flow with a clear advantage for fowler mechanism that allowed to reach higher values of maximum lift due to the effect of an increased lifting surface. Such fowler mechanism, on the other side, required even more complex kinematic actuation system due to a combination of two movements: one translation and a rotation. The fowler flap deployment mechanisms were designed using linear or curved tracks in conjunction with revolute joint for the rotation, but unfortunately, the high-lift values achieved were compensated by the relatively high weight penalties introduced by such systems. The reason for such high weight drawbacks was due to very intensive loads to be withstood by track bearings with also subsequent high maintenance costs. More recently, the research for aerodynamic efficiency and reduced weight penalties and complexity has been fostered by large utilization of multi-body system optimization that permitted the development of lighter and more efficient kinematic mechanism such as multi-link system. Such devices permit to match even very complex aerodynamic requirements with relatively structurally efficient system. As a matter of fact, today it seems very difficult to further improve in terms of an optimum balance among aerodynamic, structural weight, and complexity in the

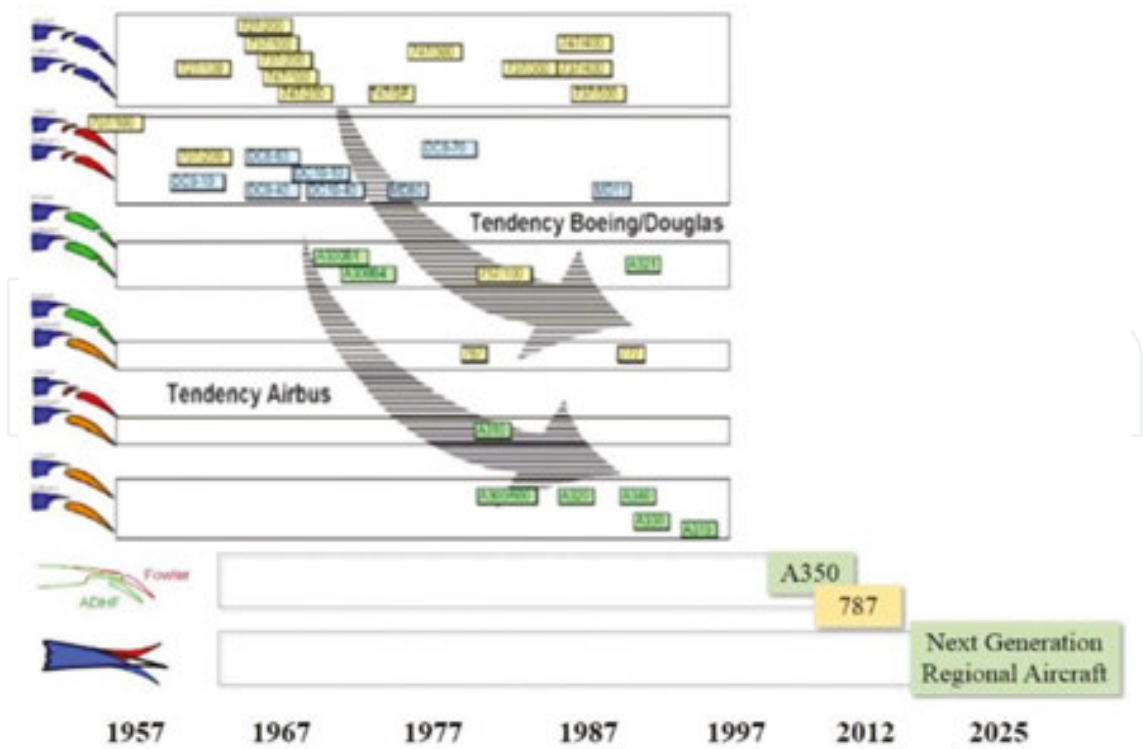
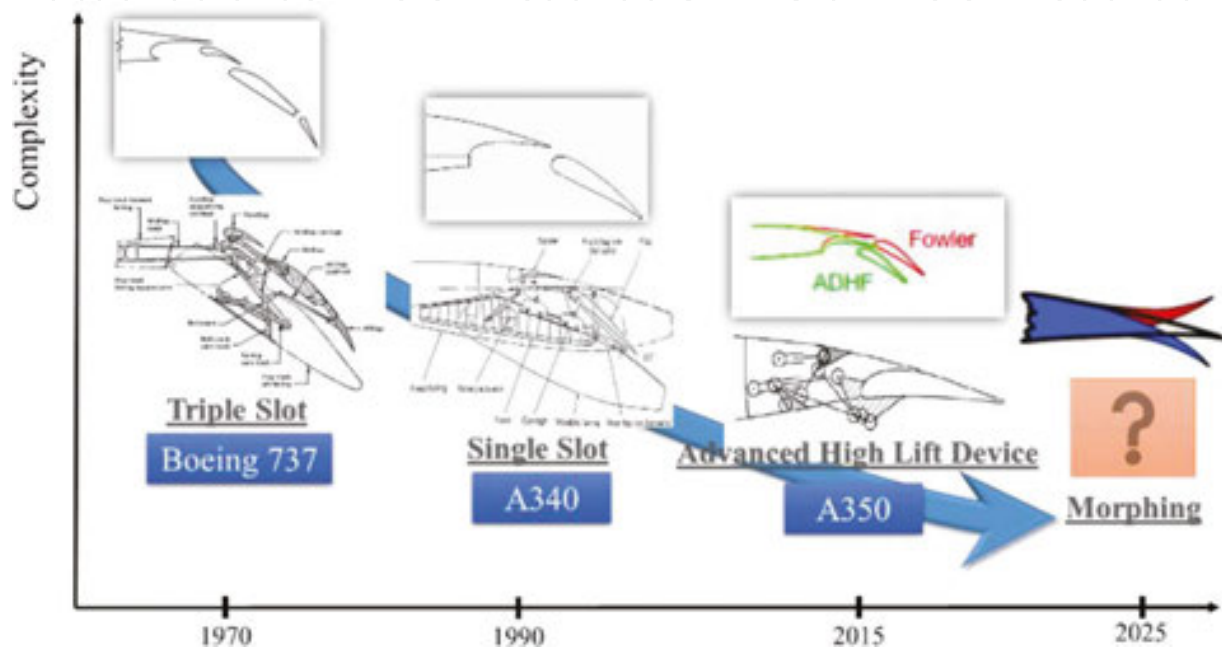


Figure 2. Evolutionary trend in high-lift systems [4].

current system, namely A350 or Boeing 767, this appears evident by the flattening of the curve in **Figure 2**.

From the previous graph, it is evident that today's high-lift system are moving toward the development of innovative mechanisms with continuous curvatures, leading to the removal of gaps in order to obtain the same performance with the less deflections. In other words, this means implementing morphing concepts, as highlighted in the graph reported in **Figure 3**.



**Figure 3.** Simplification of the high-lift actuation systems over the last few decades.

Additionally, flap mechanisms must be reliable and fail-safe. In order to not violate safety needs, the driving idea is to elude a multitude of links and joints in series, where high load concentrations are located; because the failure of any one of which could either locks up the flap, make it collapse. There are many type of flap mechanism that are largely investigated in [4, 5]. The actuation scheme of the Airbus A340 and its extraction device are depicted in **Figures 4 and 5**. The central hydraulic power control unit (PCU) supplies the power necessary to deflect the flap panels on each wing. A mechanical transmission shaft transmits the mechanical power to the rotary actuators, which move the flaps on the tracks. This shaft system consists of gearboxes necessary for larger direction changes as well as system torque limiters, wing tip brakes, universal joints, plunging joints, and spline joints to accommodate wing bending and temperature effects. The high-lift system is controlled and monitored by two slat-flap control computers (SFCC) using sensor information from several analogue and discrete sensors. This type of mechanical transmission shaft system consists of a high number of components with different part numbers and requires high design-engineering and installation effort.

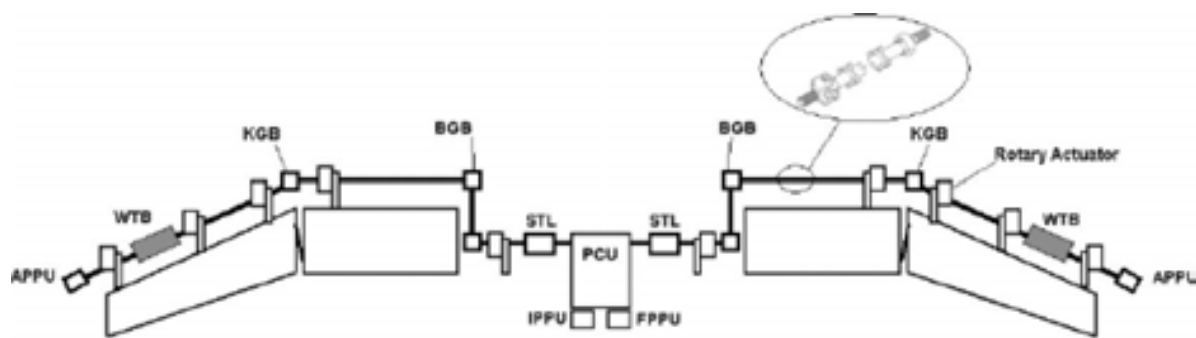


Figure 4. Global scheme of the inboard and outboard A340 flap actuation system [3].

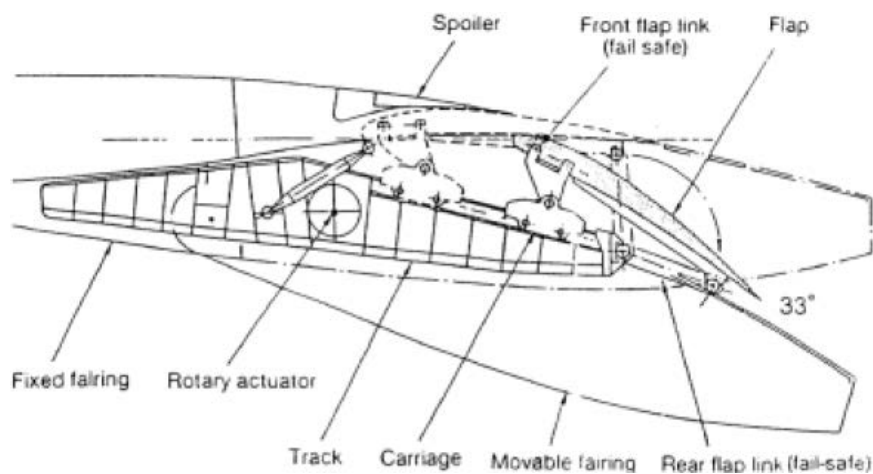


Figure 5. A340 flap mechanism based on the link/track architecture [5].

In contrast to the previous mechanism, the flap deployment system of the Boeing 767 (Figure 6) is based on a limited number of links in order to create an articulated quadrilateral or more complex hexagonal chain.

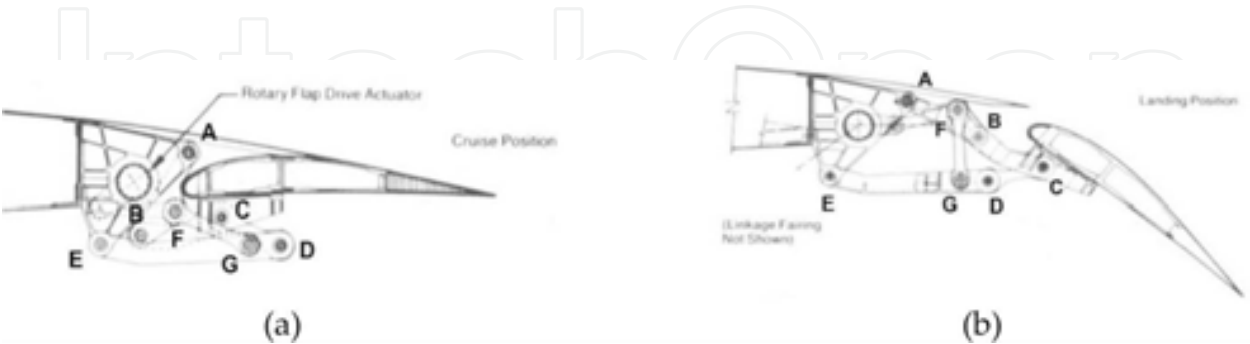


Figure 6. Boeing 767 flap system: cruise position (a) and landing configuration (b) [5].

Recent development programs at Airbus and Boeing extend the functional capabilities of the flap systems. The A350 XWB as well as the B787 high-lift systems design will incorporate additional functionalities that provide aircraft performance optimization. Additional func-

tionality is achieved with an evolution of the traditional mechanical transmission shaft system and additional active components [6]. The A350's flaps are a very simple "drop-hinge" design with a single slot between the trailing edge of the spoiler and the leading edge of the flap. As the flap extends, the spoilers deflect downwards to control the gap and optimize the high-lift performance of flap. It constitutes a multipurposes high-lift system with augmented functionalities, and furthermore, it is a lightweight structures thanks to its low complexity link-based kinematic. This can be summarized in the next **Figures 7** and **8**.



**Figure 7.** A350 XWB (Extra-Wing Body) flap in cruise condition [6].



**Figure 8.** A350 XWB (Extra-Wing Body) with A/B and tab deflection for roll control maneuver [6].

Moreover, for the first time, the flap system will have the both the capability for differential inner and outer settings as well as a variable camber function. The design is composed of a gearbox with a motor installed between the outer and inner flap that enables a differential control of the relative angle in order to shift inboard the resultant lift for a less bending moment. Furthermore, both inner and outer flaps can be moved together during the cruise to optimize the wing's camber for each phase of the flight and use the polar of drag to its most efficient configuration [6].

It remains to discuss if, as the complexity level of the actuation mechanism seems to reduce, the promise of morphing aircraft will become feasible within the next few years. If so, how morphing devices will be actuated?

The next technological challenge, envisaged in the context of more or all-electric aircraft, will be to replace the heavy conventional hydraulic actuators with a distributed spanwise arrange-

ment of smaller electromechanical actuators (EMAs). This will bring several benefits at the aircraft level: firstly, fuel savings. Additionally, a full electrical system reduces classical drawbacks of hydraulic systems and overall complexity, yielding also weight (-15%) and maintenance benefits. Lack of supply buses, improved torque control, enhanced efficiency, removal of fluid losses and flammable fluids are only some of the benefits that can be achieved. On the other hand, a general limit of electro-mechanic actuators is the possibility of jamming failures that can lead to critical aircraft failure conditions. **Figure 9** shows a practical comparison between the aircraft torque shaft configuration and a distributed actuation arrangement suitable for a morphing trailing edge device.

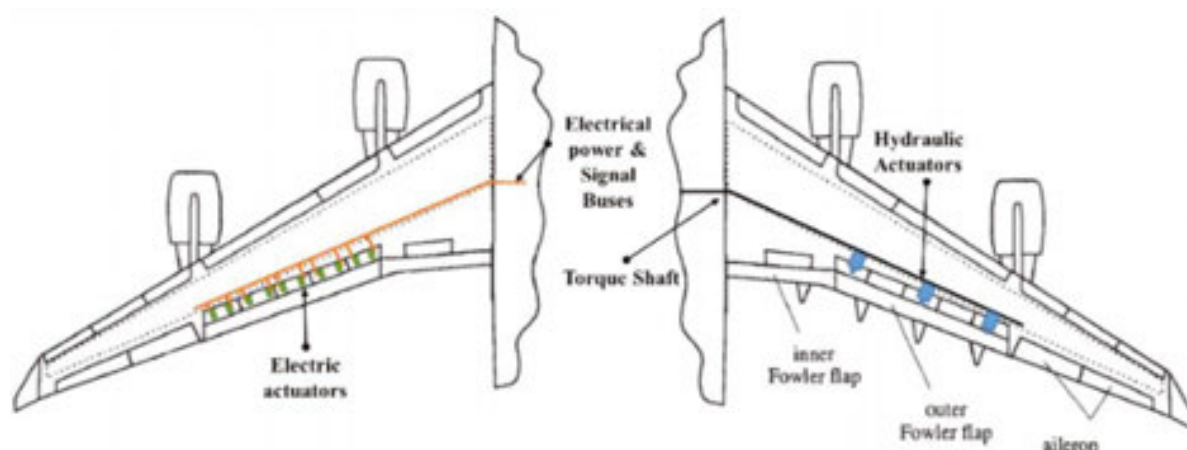


**Figure 9.** Distributed concept versus concentrated actuation concept.

The simultaneous need for monitoring target morphed shapes, actuation forces, and flight controls along with the counter-effects of aerodynamic loads under aircraft operating conditions suggests the use of a ground-based engineering tool for the physical integration of systems. The most suitable to optimize and validate such systems including electromechanical component such as actuators and flight controls is the “Iron Bird.” The basic scheme of an Iron Bird suitable for the integration of different morphing systems is depicted in **Figure 10**. It includes different morphing devices installed on an aeroelastically reasonable aircraft wing box as well as the basic equipment needed to carry out “hardware in the loop simulations.” Such a concept may be used to demonstrate advanced control technologies in a modular multi-level design that provides the robustness and the flexibility of a real aircraft integration. Manufacturing, assembly, and integration issues including electrical and flight control may be extensively addressed in relation to the actual configuration of the aircraft. It is the perfect tool to confirm the characteristics of all system components or to discover an incompatibility that may require modifications during early development stages, and thereby, it accelerates the transition to test in a relevant environment. Additionally, failures and mitigation actions introduced in the systems can be studied in full detail and recorded for analysis using such a dedicated testbed.

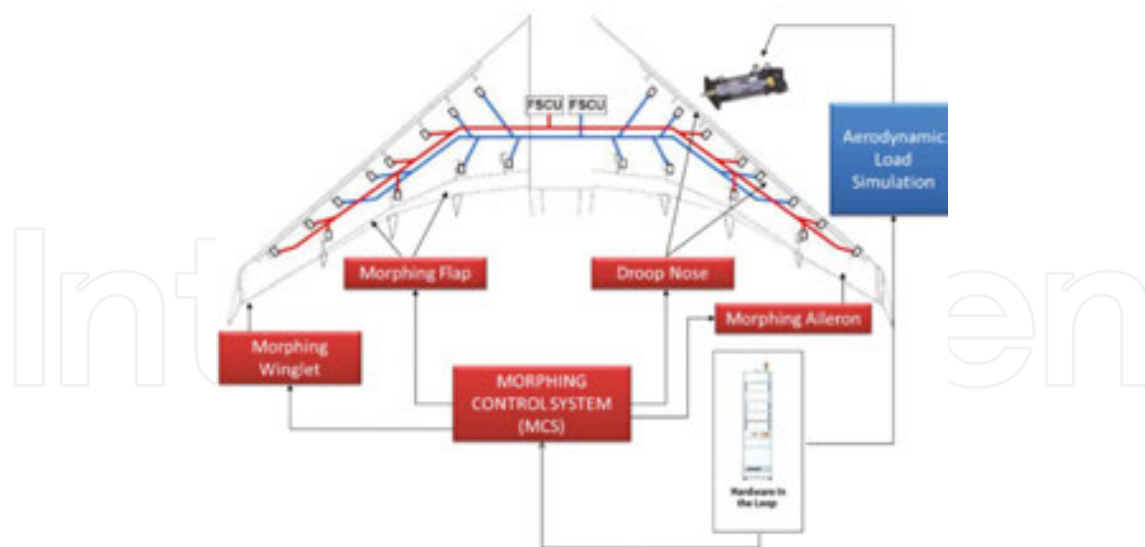


**Figure 10.** Representative scheme of an Iron Bird tool suitable for testing morphing devices.

The “Iron Bird” for testing morphing wing architectures enables test engineers to evaluate the real-time capabilities of morphing devices with the purpose of:

- demonstrating maturity, reliability, and integrated performance of morphing devices that otherwise could only be achieved with more expensive costly and less safe methods such as wind tunnel tests or flight tests;
- optimizing morphing wing architecture by testing both compliant and rigid-body mechanism-based morphing concepts and their related actuation, sensor, and control systems by monitoring aircraft weight and cost savings;
- investigating aircraft safety-related aspects by simulating system failures, such as jamming, runaways one engine loss, strong cross-wind, aeroelastic effects to validate fault tree analyses, and hazard assessments;
- including operational loads that apply hinge moment forces to the aircraft morphing surfaces, representative of the aerodynamics forces applied during the simulated flight test and driven by the flight simulation model;
- detailing cable routing and pathways;
- validating the electrical consumption of each actuation system, in stationary and dynamic conditions, and the required command to A/C surface in each test case.

## 2. Design of a morphing aileron

The design of a camber morphing aileron is following detailed as a reference case study for research into the subject. The aileron main functionalities such as roll maneuver are not modified. Conversely, with augmented capabilities integrated, the morphing aileron is

deployed in cruise, through a symmetric deflection, to obtain a near optimum wing geometry enabling optimal aerodynamic performance. The design approach, including underlying concepts and analytical formulations, combines design methodologies and tools required to develop such an innovative control surface.

### 2.1. Multi-box structure design

Inner and medium wing regions where flap systems are generally located are growingly receiving considerable attention in research. That successful development was worth to be further investigated in order to understand its applicability to the whole wing span. It does then mean to verify the applicability of those concepts to the aileron region. This region plays a fundamental role for the aircraft roll control while is subjected to the external loads. Thus, during the preliminary design phase, it is important to consider some specific critical aspects: (i) The aileron constitutes a primary control surface, which is safety critical. Failure is a catastrophic event for the aircraft; (ii) the morphing capability is added to the conventional aileron which remains free to rotate around its main hinge axis; (iii) the aileron region constitutes a delicate zone from aero-elastic point of view; (iv) morphing will introduce normal modes driving flutter instability; (v) the wing tip region is characterized by very reduced space leading to a difficult integration of actuator and kinematic. This section details the design phases of the morphing aileron, spanning from preliminary numerical verifications to wind tunnel tests. The general morphing architecture and design process resemble the same philosophy developed for the SARISTU trailing edge. The device is aimed at working in cruise to modify a limited chord segment of the aileron, so to accomplish the aircraft weight variations following fuel consumption. However, during classical maneuver, this morphing part remains rigid and the aileron works in the usual manner. Such complex adaptive system has to meet specific requirements in terms of the aerodynamic target shape, stiffness distribution, and morphing controllability. In light of these considerations, an articulated mechanism was developed, in which each component have a predominant utility, but at the same time have to cooperate with the others in withstanding loads, distributing stress and driving the architecture in a controlled way from the baseline configuration to the target shapes (morphed down and morphed up). The proposed architecture was designed according to transport regional aircraft specifications. The morphing aileron is mainly composed of: (i) five segmented rib connected by means of rotational hinges positioned on the camber line creating a kinematic chain assuring enough structural robustness and transmitting deformation; (ii) spanwise stiffening elements such as spars and stringers in a multi-box arrangements; (iii) three servo-rotary actuators which drive the mechanism; (iv) a segmented skin ("armadillo-like" configuration) with silicon gap fillers to avoid discontinuities between adjacent parts and to ensure low friction sliding during morphing.

The geometrical external contour of the aileron constitutes the first step for its structural design. The rib mechanism uses therefore a three segment polygonal line to approximate the camber of the airfoil and to morph it into the desired configuration, while keeping approximately unchanged the airfoil thickness distribution. Each aileron articulated ribs (**Figure 11**) has been assumed to be segmented into three consecutive blocks (B0, B1, and B2) connected to each

other by means of hinges displayed on the airfoil camber line (A and B) in a “finger-like” configuration. Moreover, non-consecutive rib plates are connected by mean of a link (L) that forces the camber line segments to rotate according to specific gear ratio and makes each rib equivalent to a single-DOF mechanism.

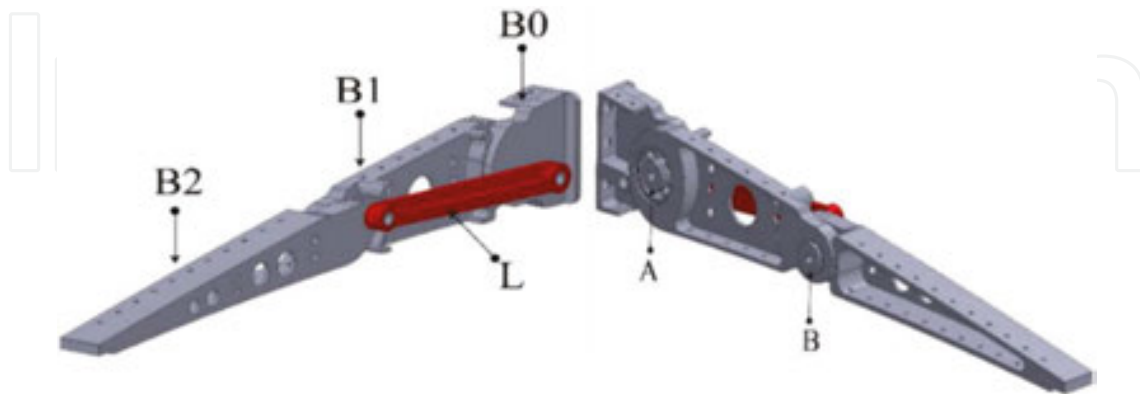


**Figure 11.** Morphing rib architecture: (a) blocks and links, (b) hinges.

The ribs’ kinematic was transferred to the overall aileron structure by means of a multi-box arrangement (**Figure 12**). Each spanwise box of the structural arrangement is characterized by a single-cell configuration delimited along the span by homologue blocks of consecutive ribs, and along the chord by longitudinal stiffening elements (spars and/or stringers). Upon the actuation of the ribs, all the boxes are put in movement thus changing the external shape of the aileron; if the shape change of each rib is prevented by locking the actuation chain, the multi-box structure is elastically stable under the action of external aerodynamic loads. A four-bay (five-rib) layout was considered for an overall (true-scale) span of 1.5 meters. AL2024-T351 alloy was used for spars, stringers, and rib plates, while 17-4PH steel was used for ribs’ links. Off-the-shelf airworthy components were properly selected for the bearing and bushings at the hinges and coupled to torsional springs to recover any potential free-play.

## 2.2. Actuation system design

The actuation system peculiarity resided in the fact that it is an un-shafted distributed servo-electromechanical arrangement deployed to achieve the aileron shape transition from the baseline configuration to a set of design target shapes in operative conditions moreover it is self-contained within the structure assuring a smooth surfaces exposed to the flow without fairing. The only kinematic mechanism that satisfies the target specifications is the oscillating glyph. The internal structure room defines the geometrical parameters which are directly related to the kinematic transmission ratio also defined as mechanical advantage (MA); furthermore, it is necessary to identify the number of actuators required to morph the aileron in particular due to small sizes near the tip, the last two bays could not be equipped with the kinematic. In **Figure 12**, it is shown that the first three ribs are drive by three individual actuators while the passive segment is slaved to the actuated one.

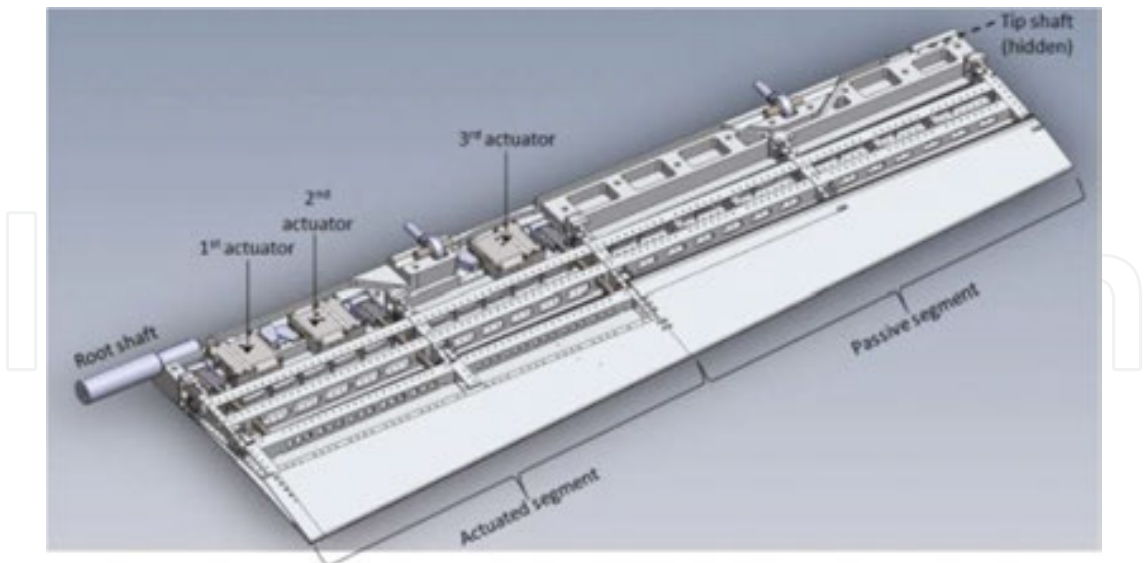


**Figure 12.** Internal view of the aileron with actuated and passive segment highlight.

A lightweight and compact leverage was investigated to activate the morphing aileron through EMAs. The deployment kinematics is based on a “direct-drive” actuation moving a beam rigidly connected to block B2 of **Figure 11**. The actuation beam transmits the actuation torque to the third segment of the rib, thus making it to rotate with respect to its original position. In particular, during morphing, the block B2 rotates around an instantaneous rotation centre. The instantaneous rotation center is here intended as the point in the moving plane around which all other points are rotating at a specific instant of time. As illustrated in **Figure 13(a)**, the trajectories of the points in the third block are all circles centered in this point. The determination of point V coordinates allows for the estimation of the actuation torque needed to withstand the aerodynamic loads acting on the morphing rib structure.

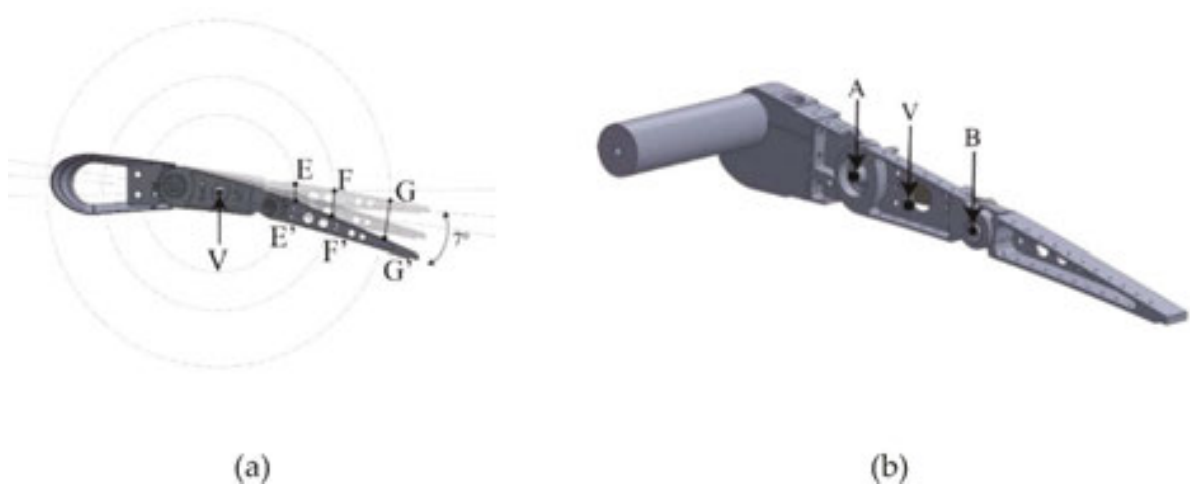


**Figure 13.** Circular trajectories of sample points (E, F, and G) during morphing (left) and position of hinges A, V, and B (right).

With reference to the **Figure 14**, the rotational motion of the actuation beam is provided by the crank rotation  $\beta$  which moves the carriage along its guide. A force  $F$  is thus generated by the contact between the carriage and the rail. By connecting the actuator shaft to the crank hinge  $O$  and the beam to the third rib segment (B2), the actuation torque is transmitted firstly to the crank and secondly to the rib rotating around the  $V$  in order to counterbalance the external moment  $M_{rib\#3}$ .

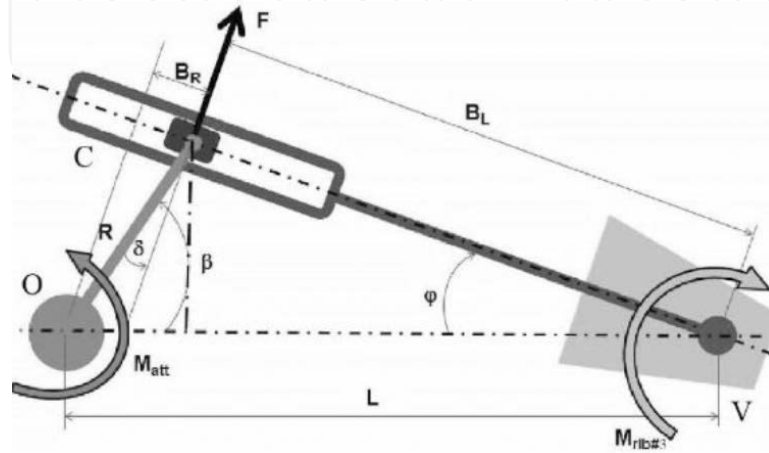


**Figure 14.** Oscillating glyph connected to the third rib segment of the morphing aileron [7].

The aileron shape can be, in this way, adaptively controlled to realize camber variations. The target morphing angles were derived as corresponding to a rigid rotation of a plain control surface comprised between  $-7^\circ$  and  $+7^\circ$ . The mechanical advantage of the mechanism (MA) can be written as follows:

$$MA = \frac{LOAD}{DRIVER} = \frac{M_{rib\#3}}{M_{att}} = \frac{F \cdot BL}{F \cdot BR} = \frac{BL}{BR} \quad (1)$$

where the  $M_{rib\#3}$  is the external moment due to aerodynamic loads estimated with respect to the hinge  $V$ , while  $M_{att}$  is the actuation torque provided by the actuator in order to equilibrate the system.  $F$  is the force that the crank produces by means of the cursor,  $BL$  is the force arm, and  $BR$  is the crank projection along the guide. Equation (2) shows that the mechanical advantage only depends on the geometrical characteristics of the system. By combining geometrical terms, it follows:

$$\cot \varphi = \frac{L}{R \cdot \sin \beta} \cot \beta \quad (2)$$

This equation allows calculating the actuator shaft rotation ( $\beta$ ) needed to achieve a given morphing angle ( $\phi$ ) of the rib block and hence of the entire mechanism. After estimating MA,

it is possible to identify the actuation torque that actuator shall supply. Accordingly, the value of the force  $F$  shall be known in order to verify that the stress arising in the carriage moving into the rail, does not exceed design allowable. The actuation rod is then subjected to the simultaneous action of the force  $F$  and the external moment  $M_{rib\#3}$ , both producing bending stress. This indicates that actuation system design requires a trade-off between the mechanical advantage and the geometrical constraints limiting the actuator shaft rotation and L/R ratio. In order to mitigate the maximum counterbalancing load acting on the guide to equilibrate the aerodynamic moment, a fork-shaped crank coupled with a double sided linear guide was preferred, as shown in **Figure 15**.



**Figure 15.** Actuation system final architecture with high rigidity linear guide.

The VLM method was adopted to evaluate aerodynamic pressure distribution along the aileron in correspondence of each considered flight attitude (namely wing angle of attack, flight altitude, and speed) and aileron geometrical configuration. The obtained loads were considered for structural sizing and validation. A linear static analysis of the isolated actuation system mechanism by means of a FE simulation was, in a first approximation, performed. The aim of the numerical simulation was to verify if the static force acting on the linear guide was below the allowable value prescribed by the producer. In the real operative condition, the linear guide, being free to move, is not subjected to stress in the direction of motion. Force is transmitted in the vertical (with respect to the guide axis) and, partially, normal direction (with respect to the guide plane). For the current application, the actuator system was sized, referring to the jamming condition, considered as the most critical. In fact, as visible in **Figure 16**, the larger extent of the constraints (additional clamps) is expected to lead to higher stresses, locally (in the contact region) and distributed (overall). The actuation beam is then simultaneously loaded with the external aerodynamic moment, the vertical static force and a horizontal component (linked to the jamming), producing a pure bending with a higher stress level rather than the free guide. This effect was simulated by means of a perfect bonding between the rail and slider. The reaction force acting on the linear guide for a given aerodynamic moment was firstly evaluated and then compared to the expected actuation torque (**Figure 17**) multiplying by the crank length.



Figure 16. Stress contour on the linear guide element (max stress ~400 MPa).

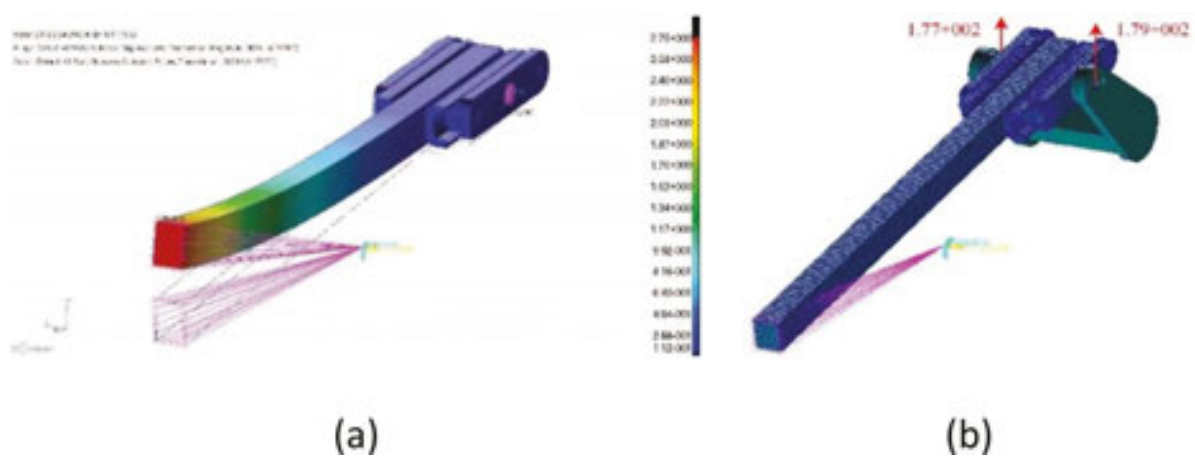


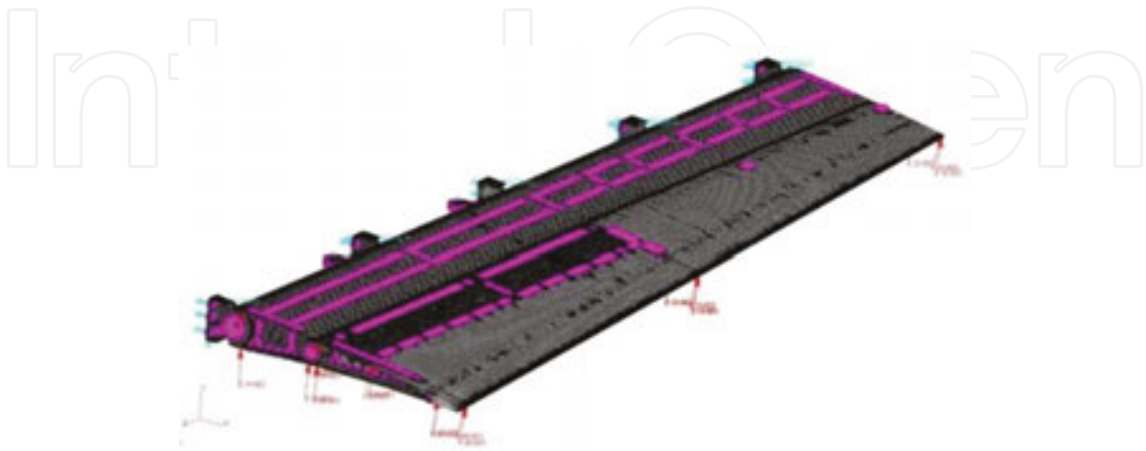
Figure 17. Beam displacement contour (a, left); guide reaction loads of 177 N and 179 N (b, right).

The finite element model of the entire aileron was then carried out. The FE model is representative of the three-dimensional drawings (CAD) of the entire aileron demonstrator. It includes main structural components such as segmented ribs and spars, actuation system leverage, and skin panels. Solid elements (CTETRA) were used for the mesh of the primary structure and the actuation leverage; meanwhile, beam elements (CBEAM) were used for modelling all the joints (fasteners, hinges, pins, and so on). FE model general data are recapped in **Table 1**.

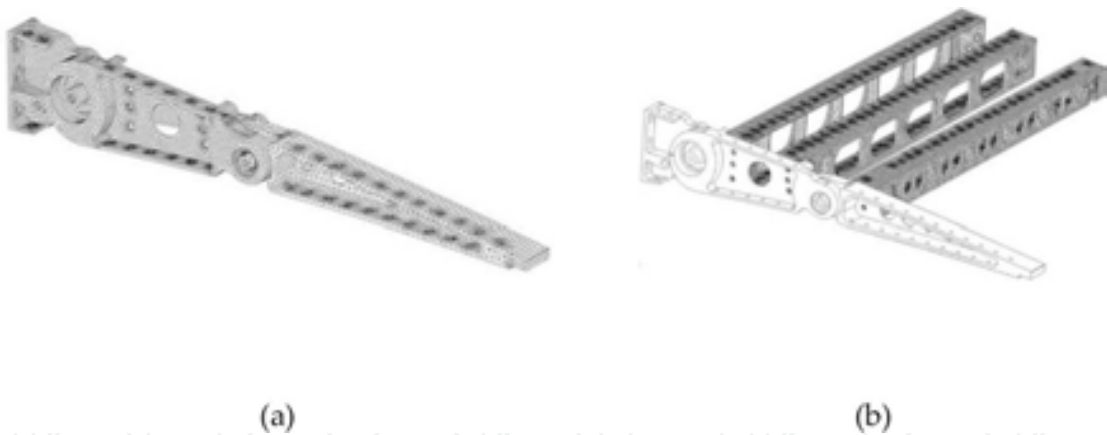
FE model general data	
Number of elements	2.138 E+6
Number of nodes	1.393 E+6
Estimated DOFs	3.638 E+6
Total estimated volume (m <sup>3</sup> )	6.785 E+6
Total estimated mass (kg)	21.00
Moment of inertia about aileron hinge-line (kg m <sup>2</sup> )	0.403

Table 1. FE model characteristics.

The aileron primary structure is composed of ribs, actuation kinematic chains, spars, and skin. Aileron leading edge was not modelled for stress analysis purposes; however, it was considered only to properly evaluate the interface loads transmitted by the aileron to the wing box. In **Figure 18**, a global view of the aileron FE model is depicted, while in **Figure 19(a)** and **(b)**, details of rib and spars meshes are shown.



**Figure 18.** Aileron FE model.



**Figure 19.** (a) Aileron rib solid mesh (CTETRA), (b) spar solid mesh (CTETRA).

Main mechanical properties of the materials adopted for the aileron components are listed in the next table (**Table 2**).

Material (isotropic)	E (GPa)	$\rho$ (kg/m <sup>3</sup> )	$\nu$	Items
Steel C50	220	7850	0.3	Beam of the actuation system, linear guide features, crank, and rib links
Al 2024-T351	70	2768	0.33	All other items

**Table 2.** Aileron components material.

All the components of the actuation system were connected to each other by means of several pins which were simulated using CBEAM elements (**Figure 20(a)** and **(b)**).

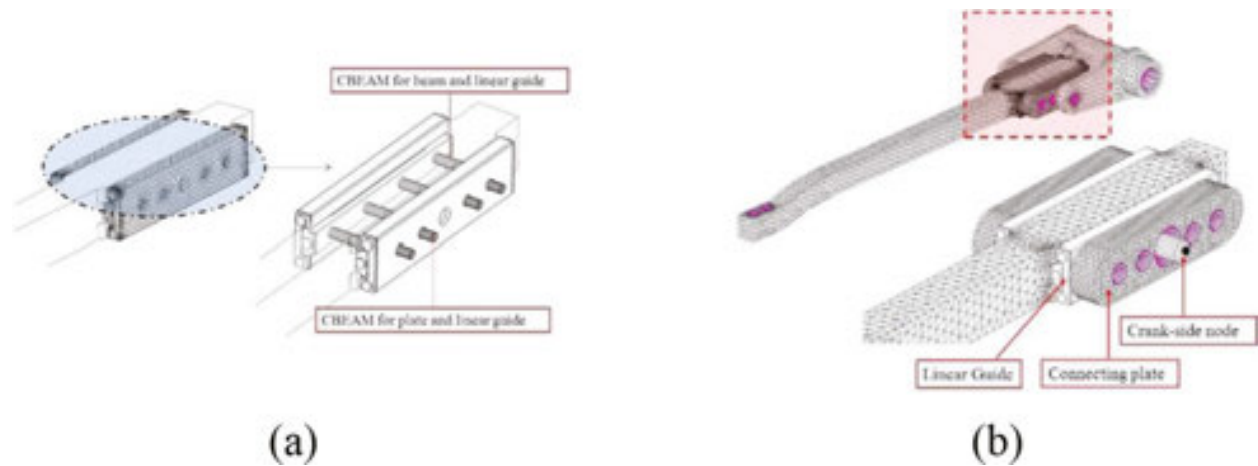


**Figure 20.** Connection pins between linear guides items (a) and detail of the local connection among the actuation kinematic parts (b).

Static analysis results have been here reported with reference to the limit load and ultimate load (1.5 times the limit load). In **Figure 21**, the global magnitude of the displacements exhibited by the aileron at limit load condition is shown. The maximum value (21.8 mm) is located at the trailing edge in proximity of the first bay.

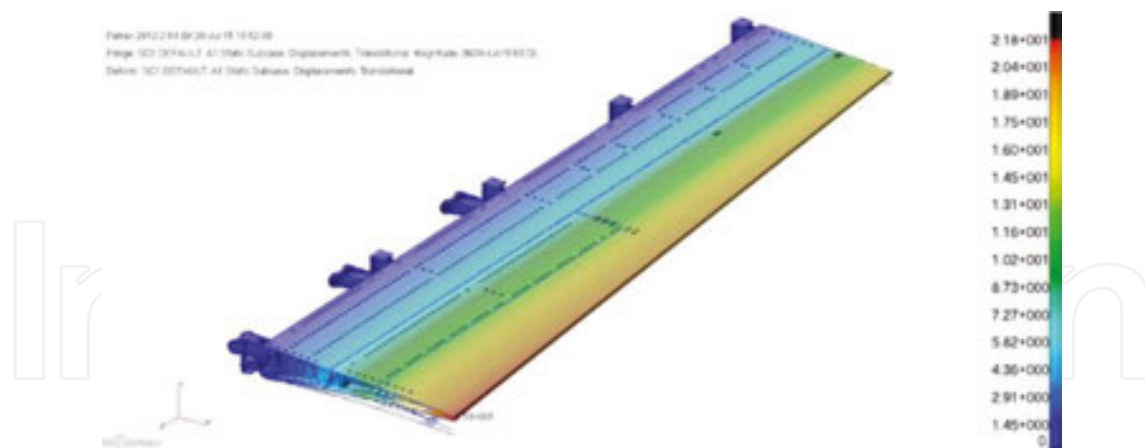


**Figure 21.** Global aileron displacement distribution at LL condition.

The stress distribution is characterized by concentrated peak around hinges and high solicitation of the actuation beam which is the most loaded components. Concerning the actuation levers, it is showed the typical stress distribution in bending; stress peaks greater than 350 MPa were found close to un-chamfered notches (**Figure 22(a)**). In addition, it is depicted (**Figure 22(b)**) the elements with stress level higher than 320 MPa. In this case, showing the most

stressed elements is localized in a small area around the holes of the linkage between beam and spar and in proximity of the linear guides.

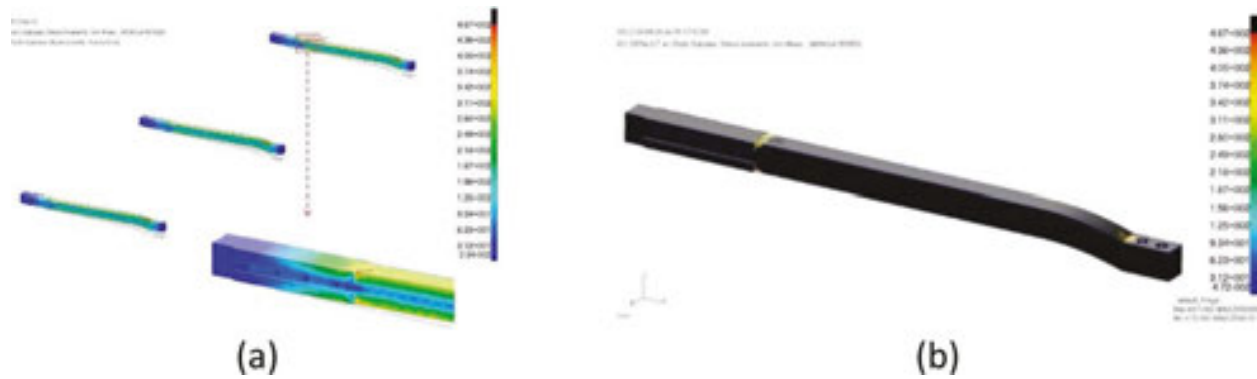


**Figure 22.** Global VM stress distribution on actuation beam at LL (a) and element stress distribution above threshold values of 320 MPa (b).

### 3. Prototyping and wind tunnel tests

On the basis of the numerical outcomes, the executive drawings of the prototype were produced and the aileron was then manufactured. Main structural parts are machined, while linear guides and actuators are components off-the-shelf (COTS). In the subsequent pictures, the segmented rib architecture, the actuation kinematic chain, and the final manufactured prototype (after painting) are shown. The morphing aileron was then integrated in a wing box and tested in wind tunnel at NRC (National Research Council of Ottawa, Canada), in the framework of the research program CRIAQ MDO505 involving Italian and Canadian university and research centre cooperation [8]. The aileron deflections are shown in **Figure 26**, and the integrated wing prototype is reported in **Figure 27**. The preliminary results obtained during wind tunnel tests were computed for baseline and morphed down configurations: lift versus angle of attack ( $CL - \alpha$ ) (**Figure 28**); drag versus angle of attack ( $CD - \alpha$ ) (**Figure 29**); drag polars ( $CL - CL$ ) (**Figure 30**). The first one shows a typical linear trend. The curve slope ( $CL_\alpha$ ) remains unchanged and clearly by a morphing aileron deflection (from baseline to  $6^\circ$ ), the camber increase (high  $\alpha_{0L}$  and the curve moves in parallel upwards. The  $CD - \alpha$  curve trend is reported in **Figure 29** for both unmorphed and morphed down configurations. The tendency shows that the minimum drag coefficient shift on the left as the morphing deflection increase leading to high  $CD_0$ . Finally, the drag polars are depicted in **Figure 30**. In this case, when a morphing deflection occur, the polar cross in correspondence of a pivot point for high  $CL$  while it moves on the right side of the Cartesian plane for low  $CL$ . This means that it is possible to identify an envelope curves which is the optimum one (dotted red line) (**Figures 23–25**).

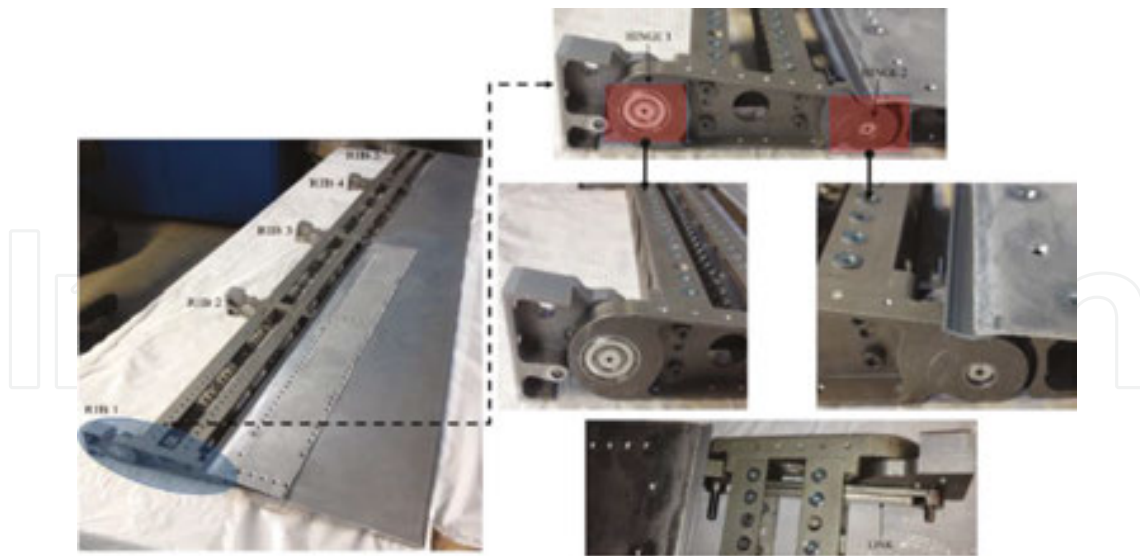


**Figure 23.** Aileron manufacturing with detail on hinges and rib.

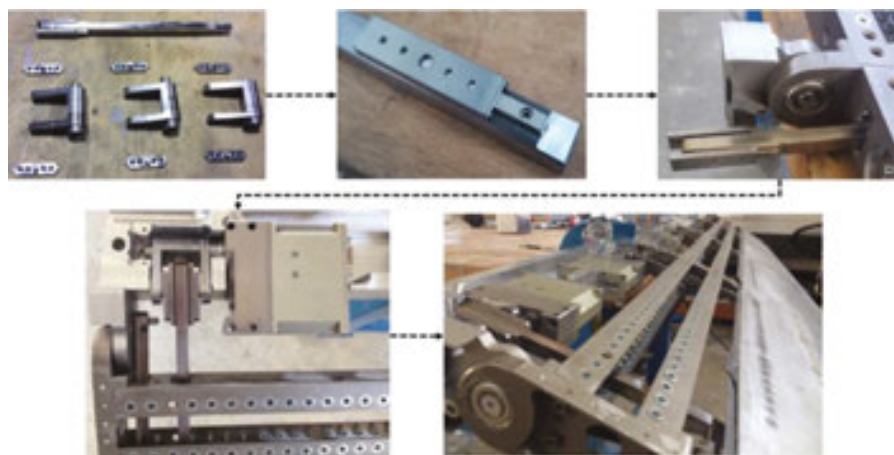


**Figure 24.** Detail on aileron actuation system.



**Figure 25.** Photograph of the aileron prototype.

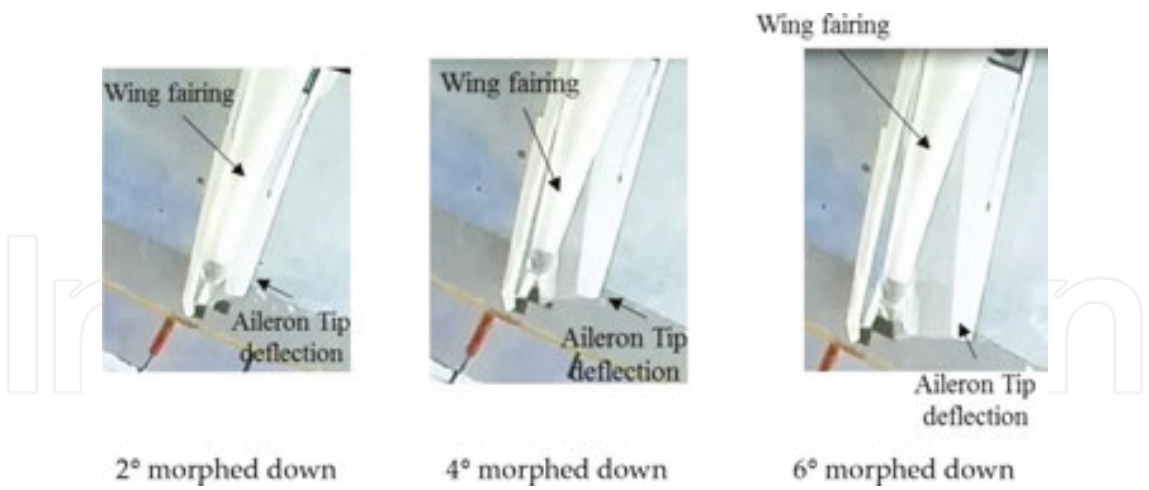


Figure 26. Morphing aileron at various deflections.



Figure 27. Complete CRIAQ wind tunnel test article including a morphing aileron [8].

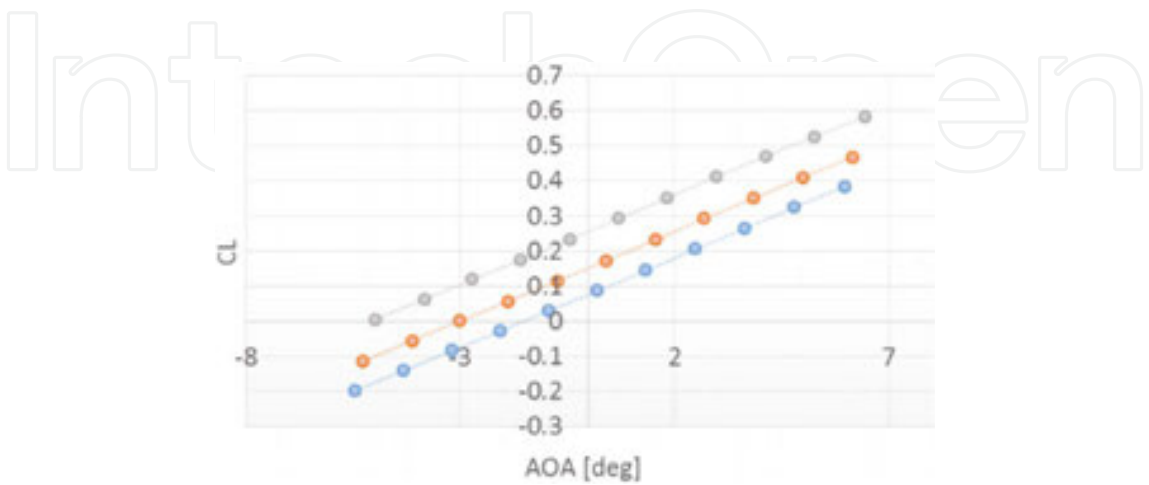
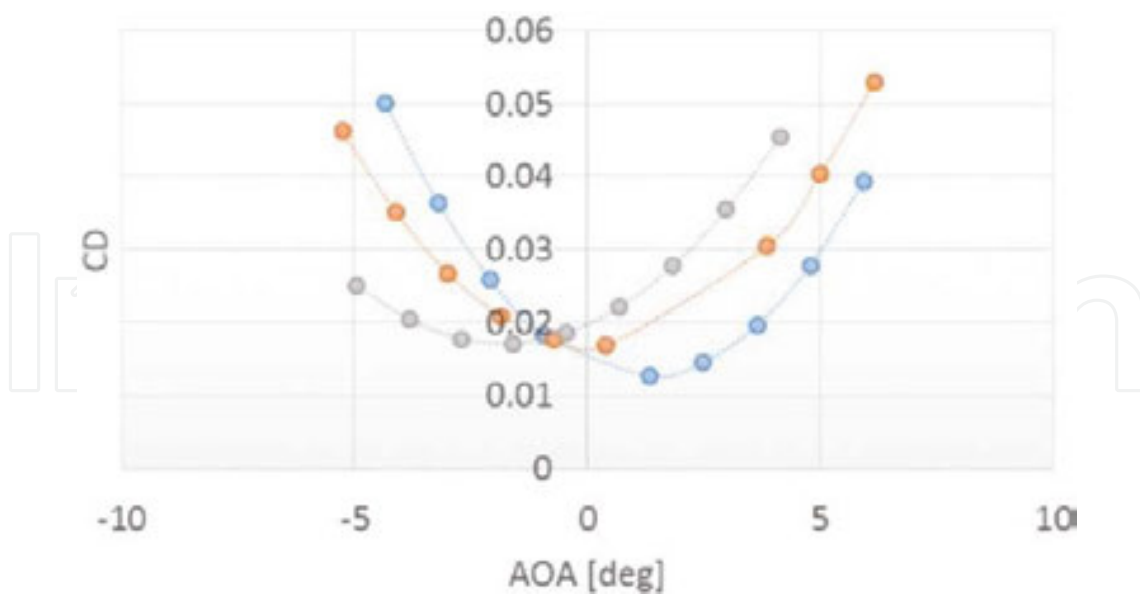
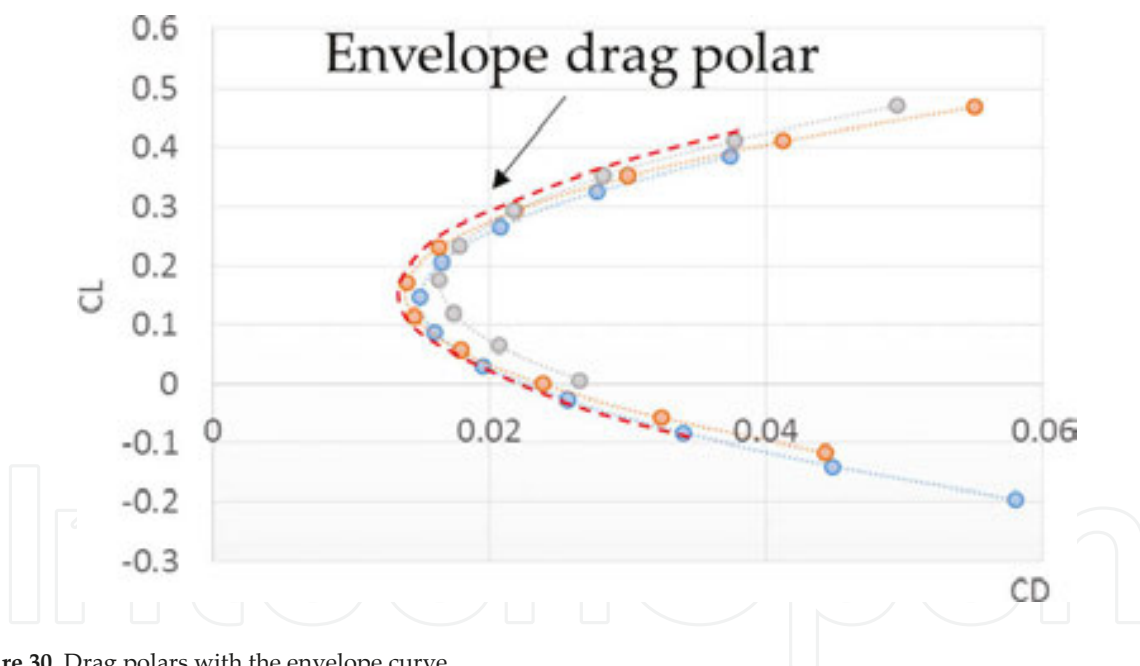


Figure 28. Lift coefficient versus angle of attack curve.



**Figure 29.** Drag coefficient versus angle of attack curve.



**Figure 30.** Drag polars with the envelope curve.

## 4. Conclusions

A self-contained morphing concept applied to a safety critical hinged control surface was presented in this chapter. In particular, a morphing aileron was investigated as an extension of an adaptive trailing edge in order to improve of  $L/D$  ratio and at the same time to preserve the conventional aileron functionality. The resulting morphed geometry, called “morphing

aileron,” ensures an augmented functionality with respect to a conventional “rigid” aileron. The device is able to rigidly rotate around main hinge axis and in addition will enable camber morphing. Being a safety critical surface, the structural design of a complete morphing aileron is rarely addressed in the literature. Such an original work provides thus evidence and arguments that contribute to the knowledge of morphing systems. Potentially suitable for static or dynamic purposes, the morphing aileron is an extension of the morphing trailing edge technology to the wing tip where small deflections could bring significant aerodynamic benefits. It has been designed for a symmetrical deflection during cruise in order to compensate A/C weight variation due to fuel burned. In such a manner, it is aimed to increase aerodynamic efficiency (reduce drag) in off design points. Additionally, the deflection of a morphing aileron it is expected to redistribute the spanwise wing distribution in order to reduce wing root bending moment. On the other hand, by increasing actuator bandwidth, it can be tailored to reduce peak stress from gust.

In order to deflect a “finger-like” rib architecture, a compact electromechanical actuation based on double-sided guides and a fork-shaped crank has been designed. Advanced finite element model in order to validate the structure at limit and ultimate loads have been carried out setting all the details necessary to produce a laboratory demonstrator. This one was assembled and tested, proving the effective functionality of the concept. Finally, wind tunnel tests assessing the aerodynamic trend of such innovative architectures have been reported. The idea herein described leads the way to further researches aimed at enhancing the TRL of the concept. To this aim, some remarks should be done on the most critical aspects of the current device. In particular, future steps may be: (i) an embedded sensing network for enhanced control in order to assure the achievement of the target aero-shapes; (ii) actual shapes evaluation and comparison with expected aero-shapes; (iii) aerodynamic benefits comparison between rigid and morphing aileron; (iv) morphing aileron-related (wing and A/C) performance benefits estimations; (v) enhanced design with topology optimization; (vi) segmented skin aerodynamics comparison with a tailored compliant skin technology; (vii) high-speed simulations and tests.

## Author details

Ignazio Dimino<sup>1\*</sup>, Gianluca Amendola<sup>1</sup>, Francesco Amoroso<sup>2</sup>, Rosario Pecora<sup>2</sup> and Antonio Concilio<sup>1</sup>

\*Address all correspondence to: i.dimino@cira.it

<sup>1</sup> CIRA, The Italian Aerospace Research Centre, Adaptive Structures Division, Capua, Italy

<sup>2</sup> University of Napoli, “Federico II”, Industrial Engineering Dept, Aerospace Division, Napoli, Italy

## References

- [1] Valasek, J., *"Morphing Aerospace Vehicles and Structures,"* John Wiley & Sons, Ltd., United States (2012)
- [2] Wölcken, P.C., Papadopoulos, M., *"Smart Intelligent Aircraft Structures (SARISTU),"* Proceedings of the Final Project Conference, Springer, Germany (2015). ISBN: 978-3-319-22413-8.
- [3] Recksiek, M., *"Advanced High Lift System Architecture with Distributed Electrical Flap Actuation,"* AST 2009, March 29–30, Hamburg, Germany.
- [4] Dreßler, U., Take-off and landing configurations, DaimlerChrysler Aerospace, March 1999.
- [5] Rudolph, P.K.C., *"High-Lift System on Commercial subsonic Airlines,"* NASA Report 4746, September 1996.
- [6] Derrien, J.C., *"Electromechanical Actuator (EMA) Advanced Technologies for Flight Controls,"* Presented at 28th International Congress of the Aeronautical Sciences (ICAS 2012).
- [7] Dimino, I., Flauto, D., Diodati, G., Concilio, A., Pecora, R., *"Actuation System Design for a Morphing Wing Trailing Edge,"* Recent Patents on Mechanical Engineering, Volume 7, 2014, pp. 138–148.
- [8] Kammegne, M.J.T., Botez, M.R., Mamou, M., Mebarki, Y., Koreanschi, A., Gabor, O.S., Grigorie, T.L., *"Experimental Wind Tunnel Testing of a New Multidisciplinary Morphing Wing Model,"* Proceedings of the 18th International Conference On Mathematical Methods, Computational Techniques and Intelligent Systems (MAMECTIS 2016).

